Analytical Methods

Accepted Manuscript

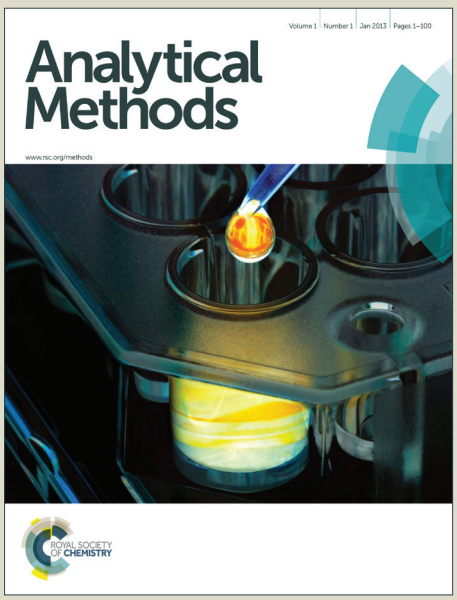

ROYAL SOCIETY OF CHEMISTRY

www.rsc.org/methods

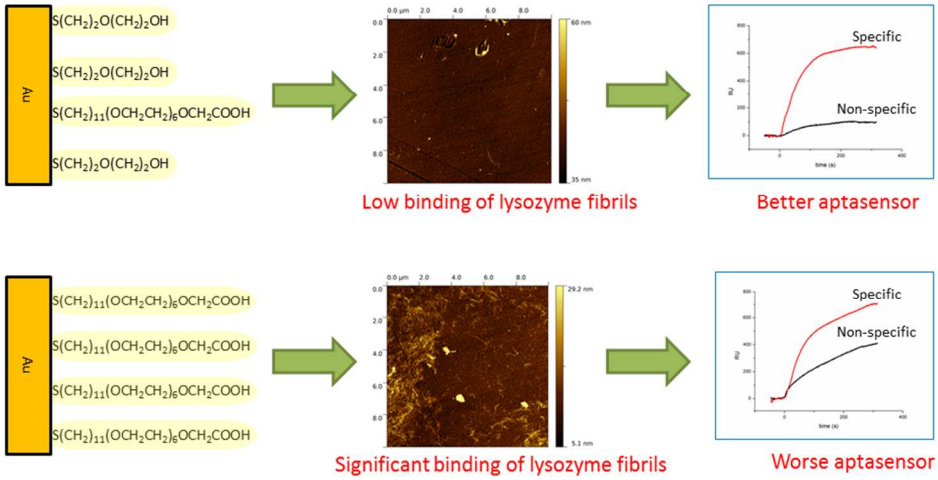

269x139mm (96 x 96 DPI)

Journal Name

RSCPublishing

ARTICLE

Low-fouling SPR detection of lysozyme and aggregates

Cite this: DOI: 10.1039/x0xx00000x

Iuliana Mihai,[a] AlisVezeanu,[a] Cristina Polonschii,[a] Sorin David,[a] Szilveszter Gaspar,[a] Bogdan Bucur,[b] Christophe Blaszykowski,[c] Sonia Sheikh,[c] Michael Thompson[c] and Alina Vasilescu[a]

Received 00th January 2012,
Accepted 00th January 2012

DOI: 10.1039/x0xx00000x

www.rsc.org/

Protein aggregates adsorb to material surfaces in a different manner than protein monomers and pose additional challenges for biosensor development with regards to non-specific adsorption (NSA). In this context, we describe herein the performance of a new antifouling thiol in a sensor coating resistant to NSA from lysozyme monomer and aggregates. Coatings were prepared as mixed self-assembling monolayers (SAM) using a long polyethylene glycol carboxyl-terminated thiol ("PEG-COOH") for the first time in conjunction with a shorter monoethylene glycol hydroxyl-terminated diluent thiol ("MEG-OH"). SAMs and their antifouling properties were characterized with a variety of surface analysis techniques. A key result was that the cleaning procedure drastically affects the anti-fouling properties of resulting MEG-OH based SAMs. Mixed PEG-COOH/MEG-OH SAMs formed on borohydride cleaned interfaces are able to reduce lysozyme NSA by > 90% compared to bare gold, a remarkable performance also displayed for oligomers regardless of their stage of aggregation. Gratifyingly, subsequent SAM functionalization with an anchoring layer of neutravidin for the preparation of a lysozyme sensor did not significantly alter the antifouling properties of the resulting assembly. The limit of detection for monomeric lysozyme by surface plasmon resonance was 0.3 µg/mL with a dynamic range of 3-50 µg/mL (R^2 = 0.9993). The sensitivity of the technique for aggregated lysozyme was almost two times higher than that for protein monomer.

Introduction

Amyloid fibrils, which are a hallmark of neural diseases such as Alzheimer's, can be studied *in vitro* using model proteins such as lysozyme. Current research encompasses two main directions, firstly, characterization of the formation of amyloid deposits together with associated toxic intermediary species[1,2] and, secondly, the screening of small molecules able to disrupt or prevent protein fibrillation[3,4]. These studies require techniques which are capable of the detection of relevant aggregated species, a difficult task considering the stochastic nature of the aggregation process.

Biosensors have emerged as an alternative to classic ELISA tests, in particular those based on EIS or SPR offering the advantage of label-free, real time monitoring of the aggregation process[5]. The architecture of typical biosensor is composed of a sensitive and specific biorecognition element (i), immobilized on a surface coating showing resistance to non specific adsorption of oligomers and fibrils (ii) and an interface that ensures sensitive detection and can be easily functionalised (iii). One key issue in these analytical devices is the availability of probes that are able to specifically bind oligomers/aggregates[6]. A popular strategy employed for the fabrication of SPR biosensors that both incorporate a probe for detection and an anti-fouling interface is self-assembling monolayer (SAM) chemistry[7-11]. With regard to the basic structure of the biosensor, although the traditionally used gold interfaces can be easily coated with SAMs of thiols, surface preparation critically influences the properties displayed by the resulting coatings. Consequently, designing a successful biosensor should consider all three aspects mentioned above.

One process that has been extensively employed as a model associated with the formation of amyloid fibrils[12-14] is the *in vitro* aggregation of hen egg lysozyme. Lysozyme is a small protein of 14.4 kDa that can be found in biological fluids such as blood, urine, saliva and tears, with the human version being associated with hereditary amyloidosis leading to liver and kidney diseases[15]. With regard to detection science and biorecognition elements, several aptamer sequences have been selected so far for this protein[16-18],

which have allowed the development of new analytical methods based on biosensor technology[19-21]. However, as is the case for many biosensors, a major challenge for application of the protein is the non-specific adsorption problem. (Interestingly, lysozyme, which has a high isoelectric point (pI=11) and is positively charged over a wide pH range, has been used widely as a model protein in terms of the characterization of materials capable of the resistance of fouling[7,22].

Among the many different types of such surface modifiers reported over the years to form antifouling coatings, long-chain PEG-based constructs constitute historically the gold standard to prepare so-called bio-inert surfaces[23-27], although the mechanism that lies behind the efficacy of such chemistry is still the subject of debate. More recently, it has been demonstrated that significantly shorter chain monoethylene glycol (MEG-OH) surface modifiers can be employed successfully in order to reduce fouling[9,28].

In the present paper, we report the development of a new sensor coating based on a SAM formed from a binary mixture of thiolated MEG-OH and a long carboxyl-terminated thiol, incorporating six ethylene glycol groups, the latter being used to attach an aptamer. Coatings were characterized by a variety of surface analysis techniques including contact angle goniometry, cyclic voltammetry, electrochemical impedance spectroscopy and atomic force microscopy. The antifouling properties of the MEG-OH SAM with respect to the adsorption of lysozyme monomer and aggregates was measured using surface plasmon resonance (SPR). An application for the detection of lysozyme aggregates based on specific recognition using an aptamer is also included.

Experimental

Reagents

Lysozyme (from chicken egg white) was purchased from Sigma-Aldrich. The thiol 32-mercapto-3,6,9,12,15,18,21-oxa-dotriacontanoic acid ($HS(CH_2)_{11}(OCH_2CH_2)_6OCH_2COOH$, "PEG-COOH") was purchased from Prochimia Surfaces – Poland. 5-mercapto-3-oxa-pentanol $HS(CH_2)_2O(CH_2)_2OH$ ("MEG-OH") was synthesized at the University of Toronto, Department of Chemistry (Toronto, Ontario, Canada) and characterized elsewhere [27]. Hydrogen peroxide was purchased from Carl Roth, potassium hexacyanoferrate (III) from Merck, aluminum oxide powder (0.35-0.49 μm particle size) from Alfa Aesar and neutravidin from Pierce. The lysozyme aptamer – with the 5'-GGG AAT GGA TCC ACA TCT ACG AAT TCA TCA GGG CTA AAG AG-3' sequence including a 24 base polythymine linker and biotinylated at the 5' end – was obtained from Integrated DNA Technologies. All other reagents were from Sigma-Aldrich and used as received unless otherwise noted. Lysozyme oligomers were produced from a 10 mg/mL solution of lysozyme subjected to forced aggregation according to a previously described protocol[29]. Aliquots taken at several time intervals from this solution corresponded to different stages of aggregation.

SAM preparation

Gold electrodes for electrochemistry experiments (Metrohm, 3 mm in diameter) were polished with aluminum oxide powder, ultrasonicated in ethanol for 20 s and then immersed in hydrogen peroxide for 15 min. An electrochemical cleaning was next carried out by cyclic voltammetry in 0.5 M H_2SO_4 (from -0.4 to +1.6 V with a scan rate of 100 mV/s) for at least 15 cycles – until the typical voltammogram of clean gold was observed.

Gold chips for SPR analysis were cleaned using two different procedures. In the first protocol, chips were kept for 24 h in a 1:10 hypochlorite aqueous solution, then for 10 min in a 0.5 M $NaBH_4$ solution (prepared in a 1:1 mixture of water and ethanol). In the second protocol, chips were also initially kept for 24 h in a diluted hypochlorite solution (1:10), followed by 10 min in a 1:1 NaOH: H_2O_2 mixture, then 10 min in acetone.

After rinsing several times with copious amounts of water and ethanol, gold electrodes and chips were dried under a gentle stream of nitrogen then immersed immediately in one of the following thiol solutions prepared in ethanol: 1) 1 mM MEG-OH for 30 min, 2 h or 2 days; 2) 50 μM PEG-COOH for 2 days; or 3) PEG-COOH/MEG-OH (1:20) for 2 days.

Instrumental characterization

Static contact angles (CA) were measured with a CAM 100 goniometer (KSV Instruments) and water as the test liquid. CA values were generated using the *CAM 100* software.

Gold surfaces, bare or modified with either a PEG-COOH or a PEG-COOH/MEG-OH mixed SAM were studied by atomic force microscopy subsequent SPR detection of lysozyme aggregates. This protocol allowed a direct comparison of SPR response with actual physical NSA. AFM scans were obtained in air using a Nanowizard II AFM instrument (JPK) operating in tapping mode with an Arrow NC cantilever (NanoWorld AG, ~285 kHz resonant frequency, ~ 42 N/m constant forces).

Electrochemical detection

All experiments were performed using a VSP potentiostat/galvanostat from Bio-Logic S.A (France) equipped with *EC-Lab* software. A classic 3 electrode setup was employed that included an Au working electrode, a Pt counter electrode and a Ag/AgCl, KCl (3 M) reference.

Cyclic voltammetry (CV) was performed in a cell containing 1 mM $K_3[Fe(CN)_6]$ in phosphate buffered saline (PBS) pH 7.4 from -0.2 to +0.6 V with a scan rate of 100 mV/s. Electrochemical impedance spectroscopy (EIS) was performed in PBS pH 7.4 containing 1 mM $K_3[Fe(CN)_6]$ and 1 mM $K_4[Fe(CN)_6]$, at the formal potential of this redox couple on a clean gold electrode (~ 0.220 V *vs*. Ag/AgCl, 3 M KCl) over which was applied a sinusoidal signal with an amplitude of 10 mV and frequency range from 9.5 kHz to 1 Hz. Data were fitted with a Randles equivalent circuit using the *Z Fit* software included in the *EC-Lab* package. Electrodes for EIS analysis were exposed for 15 min to a 1 mg/ml lysozyme solution in PBS pH 7.4, then rinsed with distilled water for 5 min under magnetic stirring. EIS measurements were also performed before incubation.

Surface plasmon resonance detection

SPR measurements were performed on a modified Spreeta TSPR2K23 sensor (Texas Instruments). The system was equipped with a two-channel polydimethylsiloxane flow cell, which allows for delivery of the analyte solution to the sensing surface. Details and fabrication of the SPR chips are described elsewhere[30]. Two buffer solutions were used for testing the NSA of lysozyme and oligomers: (1) PBS pH 7.4 and (2) 20 mM Tris–HCl pH 7.4 with 100 mM NaCl and 5 mM $MgCl_2$. SAM-coated gold chips were first allowed to equilibrate with running buffer for 20-30 min at 100 μL/min. NSA measurements were then carried out in two different ways. First, a fresh solution of 1 mg/mL lysozyme in PBS was injected for 15 min at a rate of 30 μL/min. Next, the SPR cell was rinsed for 10 min with PBS buffer (100 μL/min). The difference in baseline before injection of lysozyme and after rinsing with buffer (ΔRU) was considered as an indicator of NSA. Second, solutions of lysozyme and oligomers

(30 µg/mL in TRIS buffer pH 7.4) were injected for 5 min at 100 µL/min. The SPR cell was next rinsed with running buffer for another 5 min at the same flow rate. The difference in baseline before protein injection and after rinsing (ΔRU) was considered as an indicator of NSA. For experiments involving successive sample injections, sensing surfaces were regenerated on-line with short pulses of 50 mM NaOH and 0.1 M glycine pH 2, until the SPR signal returned to its original baseline. In order to obtain lysozyme oligomers, a 10 mg/mL solution of lysozyme was subjected to forced aggregation according to a previously described protocol[29]. Aliquots taken at different time intervals corresponded to different stages of aggregation. For calibration with various concentrations of lysozyme (0.1 to 200 µg/mL), measurements were performed for 5 min at a flow rate of 100 µL/min.

Results and discussion

Non-specific adsorption of monomeric lysozyme

Prior to investigation of lysozyme adsorption, the chemistry of the thiol species on gold was examined. The changes in electrochemical properties of gold upon modification with both short and long-chain thiol SAMs measured by CV and EIS are illustrated in Figs. 1 a and b.

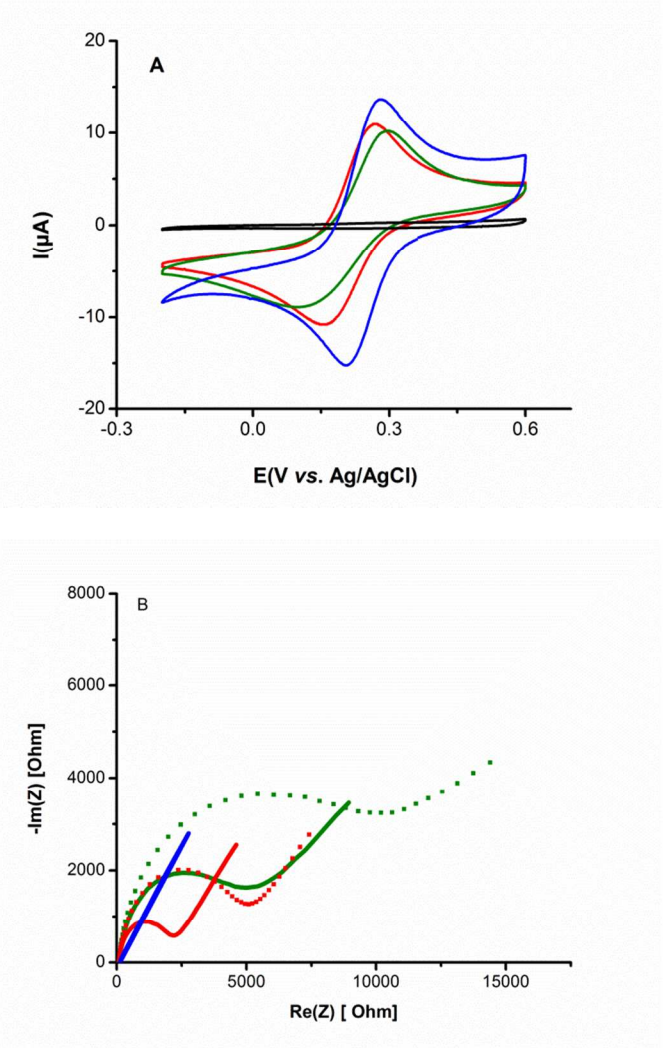

Figure 1. a) Cyclic voltammograms of a 1 mM potassium ferricyanide solution in PBS for cleaned, bare (blue), MEG-OH SAM-coated (red), PEG-COOH/MEG-OH mixed SAM-coated (green) and PEG-COOH SAM-coated gold electrodes (black). The immersion time for SAM formation was 48h. **b**) EIS Nyquist plots for cleaned, bare gold (solid blue), MEG-OH SAM before (solid red) and after (dashed red) exposure to lysozyme, as well as PEG-COOH/MEG-OH mixed SAM before (solid green) and after (dashed green) exposure to lysozyme. Incubation conditions were 15 min in PBS pH 7.4 with a lysozyme concentration of 1 mg/mL.

Compared to the expected fast electron transfer of ferricyanide on a bare gold electrode, the separation between oxidation and reduction peaks (ΔE_p) increases for electrodes coated with MEG-OH and mixed PEG-COOH/MEG-OH SAMs from 72 (± 1) mV to 119 (± 3) mV and 187 (± 67) mV, respectively. The higher resistance to electron transfer due to the presence of intercalated MEG-OH or PEG-COOH/MEG-OH SAMs was also reflected in evident changes in the EIS spectra (depicted in the Nyquist plot, Fig. 1b). Impedance data were fitted with a classic Randles equivalent circuit encompassing bulk solution resistance (R_S), constant phase element (CPE – models the electrical double layer at the electrode-solution interface), Warburg impedance (W – accounts for the diffusion of active species to the electrode surface) and charge-transfer resistance (R_{CT}) components.

Upon SAM formation, the impedance alters (Fig. 1b), the R_{CT} being the most sensitive parameter to interfacial changes. As expected, monomolecular MEG-OH coatings display significantly lower R_{CT} compared to mixed coatings obtained by incorporation of the long PEG-COOH thiol (2089 ± 787 Ω and 4548 ± 842 Ω respectively). Thus, the variation of R_{CT} upon adsorption of lysozyme was taken as an indicator of non-specific adsorption.

Table 1. Changes in optical (ΔRU) and electrochemical (ΔR_{CT}) properties respectively measured with SPR and EIS for bare and various SAM-coated gold surfaces upon incubation with lysozyme.

Coating	SAM formation (h)	SPR	EIS
		ΔRU	ΔR_{CT} (Ω)
bare gold	0	757 ± 148	39191 ± 10999
MEG-OH	0.5	307 ± 112	3928 ± 615
MEG-OH	2	389 ± 193	3672 ± 202
MEG-OH	48	286 ± 125	2785 ± 717
PEG-COOH/MEG-OH	48	486 ± 31	2375 ± 610
PEG-COOH	48	191 ± 36	N/A*

* The R_{CT} value for the monomolecular PEG-COOH SAM was so large, already before incubation with lysozyme,that accurate faradaic EIS measurements could not be performed[31].

Table 1 shows the increase in R_{CT} upon adsorption of lysozyme on the thiol-coated surfaces is very small (< 10%) compared to bare gold. Together with SPR results, summarized in Table 1, the results show an obvious, efficient reduction of lysozyme NSA upon coating the gold interfaces with either monomolecular MEG-OH, PEG-COOH or mixed PEG-COOH/MEG-OH SAMs. The adsorbed protein amount estimated by SPR[32] (1RU corresponds to 1 pg protein/mm^2.) is lowered by 36-75% (Table 1) compared to unmodified gold. The antifouling behaviour of the thiol containing a single ethylene glycol group is remarkable and consistent with

previous work[33]. This result stands in contrast with the prevailing view that the antifouling capacity of SAMs increases significantly with the number of ethylene glycol groups[34].

With regard to the time of formation of SAM, the data in Table 1 reveal that the resistance to protein adsorption provided by the monomolecular MEG-OH SAMs produced after 48h, 2h or only 0.5h is not significantly different, suggesting that MEG-OH SAM formation occurs rapidly. Additionally, analysis of EIS data by ANOVA shows that mixed PEG-COOH/MEG-OH SAMs have similar low-fouling properties as monomolecular MEG-OH SAMs as judged from the observed changes of the resistance to charge transfer at the interface.

Finally, with regard to the NSA behaviour of SAMs on gold it is necessary to discuss experiments we conducted on the role played by cleaning procedures employed for the metal. Data regarding systematic investigations of cleaning procedures for SPR chips is scarce. The procedures typically used for cleaning gold electrodes are either too aggressive or difficult to implement with thin (50 nm) gold films[35]. A recent report found that cleaning in oxygen plasma lead to better SPR transducers than surface pre-treatment with organic solvents, piranha or KOH[35]. On the other hand, a "milder' method has been described for the cleaning of Au nanoparticles[36], which is based on the use of sodium borohydride. We hereby investigated two different approaches for cleaning SPR interfaces: (1) a reducing treatment using sodium borohydride ($NaBH_4$)[36,37] and (2) a basic, oxidative treatment using a mixture of sodium hydroxide and hydrogen peroxide[38]. Contact angle goniometry revealed that cleaned gold SPR chips displayed a rather pronounced hydrophobic character with contact angles of 87 ± 2º (n = 3) and 76 ± 2º (n = 3) upon $NaBH_4$ and $NaOH/H_2O_2$ treatments, respectively. In comparison, the coatings – which present distal OH and/or COOH polar groups – were more hydrophilic with contact angles of respectively 27 ± 7º and 37 ± 1º for the monomolecular PEG-COOH and MEG-OH SAMs, and 42 ± 4º for the PEG-COOH/MEG-OH mixed SAMs.

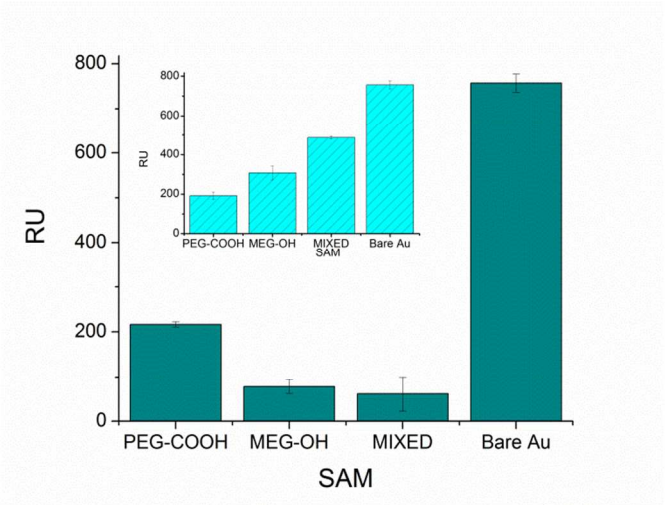

Figure 2. SPR signal due to adsorption of 1 mg/mL lysozyme at pH 7.4 on gold surfaces cleaned with $NaBH_4$ and coated with SAMs formed from MEG-OH, PEG-COOH and a mixture of 1: 20 PEG-COOH/MEG-OH thiol. Inset: results for surfaces cleaned with NaOH: H_2O_2, prior to immersion in thiol. Non-specific signal of lysozyme on clean gold was 750 ± 216 RU

Importantly, the $NaBH_4$ treatment proved very effective, as compared to the $NaOH/H_2O_2$ procedure (Fig. 2), for promoting the formation of MEG-OH-modified surfaces that reduce the level of lysozyme NSA. This was not the case for PEG-COOH SAMs, a result which implies that the properties of oligoethylene glycol thiol SAMs with six ethylene glycol groups are not influenced by the surface density of the thiols, as contrasted with SAMs containing a lower number of EG groups.[39]

3.2 Adsorption of lysozyme aggregates

Protein aggregation is a complex dynamic process which represents a difficult challenge in terms of the detection of physical chemistry of species formation. In the present work, aggregation of lysozyme was induced in acidic conditions at high temperature as per a previously described protocol[29].

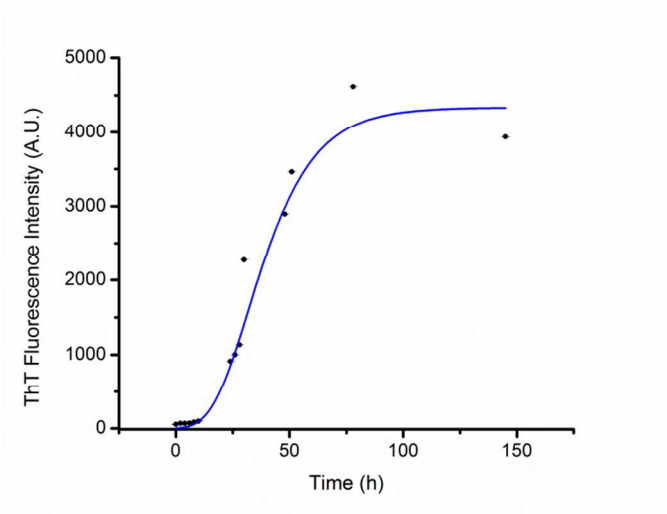

Figure 3. Progress of lysozyme aggregation monitored by Thioflavin T fluorescence.

Fluorescence spectroscopy performed with thioflavin T (Fig. 3) showed that the signal increases upon formation of fibrils due to the binding of the dye to the grooves of the beta-sheets in amyloid fibrils[40]. Using AFM, we show that solutions aggregated for 48 h contain protofibrils that adsorb significantly to both bare gold and PEG-COOH SAMs (a surface chemistry that satisfactorily resisted to NSA from protein monomers). This behavior is in stark contrast to the one observed for the PEG-COOH/MEG-OH mixed SAM for which protofibrils have low affinity (Fig. 4).

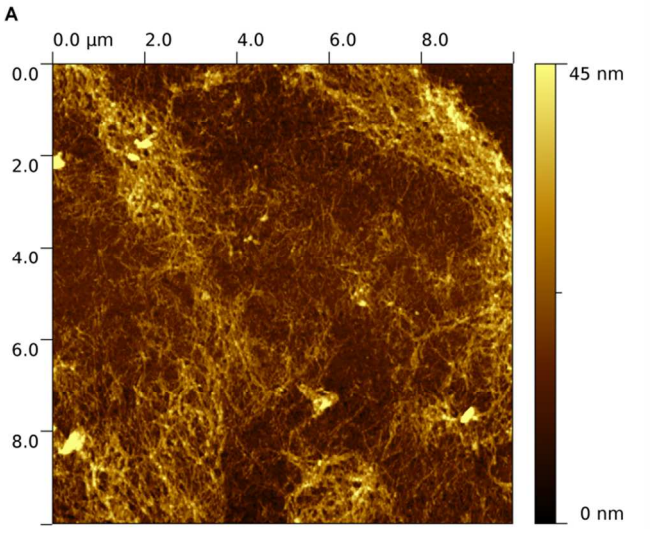

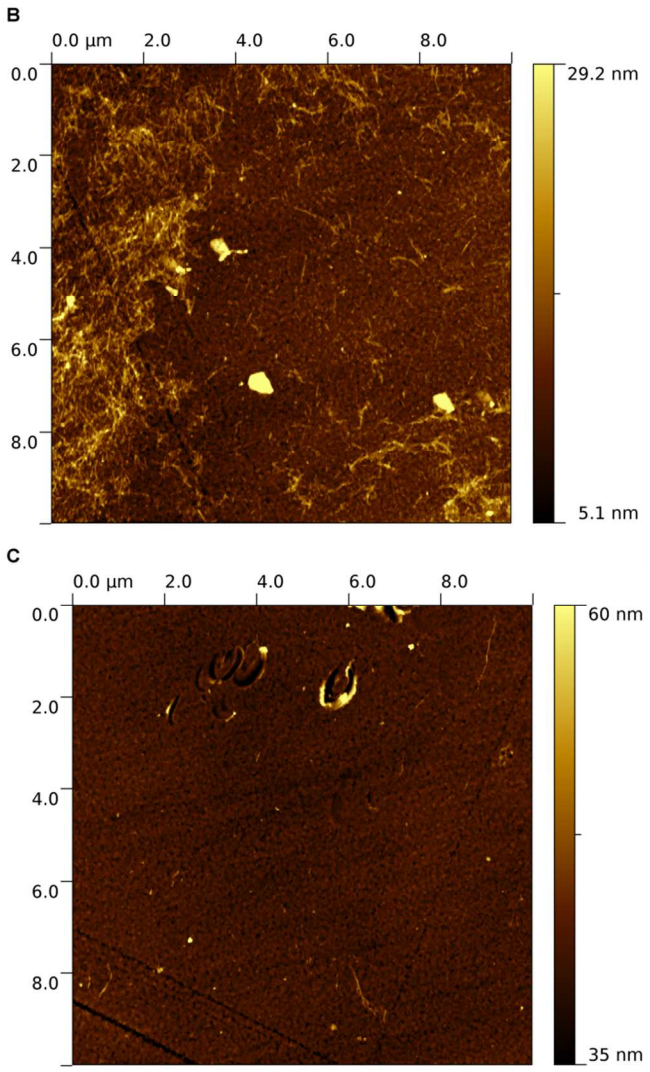

Figure 4. AFM analysis showing protofibril adsorption on bare (A), PEG-COOH SAMs (B) and PEG-COOH/MEG-OH mixed SAM-coated (C) gold surfaces, submitted to a solution of lysozyme aggregated for 48 h.

Compared to the monomer, lysozyme aggregates appear to expose new amino acids to their environment and, thus, adsorb to the sensor surface through a different mix of interactions. These are counteracted by the PEG-COOH/MEG-OH mixed SAM but not by the PEG-COOH SAM. It has been shown that native and aggregated protein present different affinities towards polyanions. Indeed, polyanions can increase the aggregation rate, bind tightly to preformed fibrils, and stabilize the aggregated state of proteins (through compensation of electrostatic repulsion[41]. On the other hand, the pKa of ω-carboxyl alkane thiols increases when such thiols are self-assembled into monolayers[42,43] and carboxylic acid-ended SAM display multiple bridged/unbridged structures at a water interface[44].

SPR-aptamer based selective detection of lysozyme and aggregates

Prior to selective detection experiments using SPR a measure of quality assessment of commercial SPR chips, based on calculation of a quality parameter Qp[45], was conducted involving quantification of changes in SPR signals over time (Fig. 5).

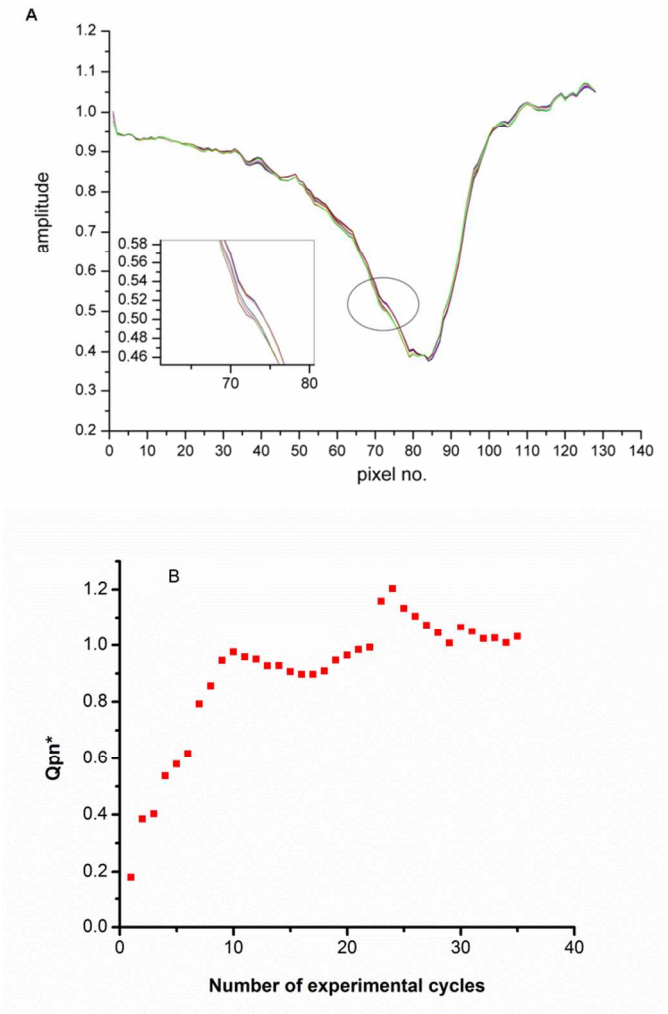

Figure 5. Evolution of the SPR curves (A) from which the quality parameter Qp was calculated[45], with repetitive measurements during 4 days (B).

This evaluation leads us to conclude that only very small changes occur in the SPR curve (and by consequence in the properties of the interface) after the first day of use. The sensor interface could be used for 3 days without significant loss in performance.

The design employed for the development of an SPR aptamer-based detection system for the protein and aggregates is depicted schematically in Fig. 6 and was described in detail elsewhere[29]. In summary, this involves using a base of a mixed SAM followed by *on-line* attachment of the coupling agent for the probe, in this case, neutravidin. (The latter is bound to the SAM via well-established carbodiimide coupling chemistry[46].) Further on, the attachment of lysozyme aptamer is also done in flow, exploiting the strong affinity interaction between the biotinilated aptamer and the neutravidin surface. The SPR system comprises two channels, only one being modified with aptamer while the other was kept unmodified as reference, for the evaluation of NSA and of any variations in the analytical system.

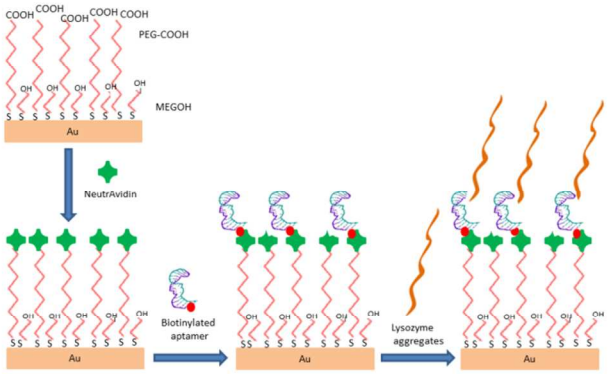

Figure 6. Schematic representation of SPR-aptamer device construction: (1) Au interfaces coated with mixed SAM; (2) functionalization with Neutravidin; (3) immobilization of biotinilated aptamer; (4) analysis of lysozyme and aggregates

Neutravidin is very useful agent for the attachment of biotinylated probes to device surfaces. While some reports found that neutravidin-functionalised interfaces display high resistance to cellular NSA[47], others observed that such functionalization may cause NSA to significantly increase[48]. Consequently, we found its necessary to assess the nature of interaction of a neutravidin-modified SPR chip with both lysozyme oligomers and monomeric lysozyme (Fig. 7). It is noteworthy that NSA of aggregated lysozyme solutions was remarkably low even for samples aggregated for 3 days, as opposed to previous results with a monomolecular PEG-COOH SAM[29]. In that study, although the thiol proved successful in terms of repelling monomeric lysozyme and other proteins, the non-specific adsorption displayed by aggregated solutions was at a significant level. This discrepancy was confirmed by AFM as described in section 3.2.

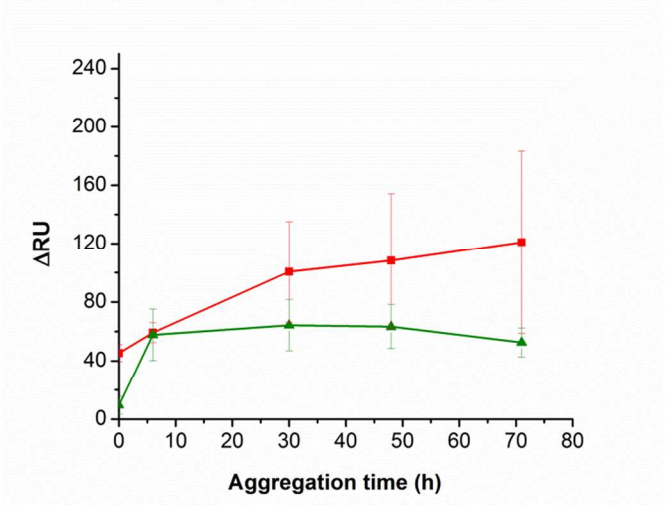

Figure 7. Variation of the SPR signal due to NSA of lysozyme and oligomers on unmodified PEG-COOH/MEG-OH mixed SAMs (green) or functionalized with neutravidin (red) as a function of forced aggregation time (t = 0 corresponds to monomeric lysozyme).

With respect to selective binding onto aptamer-functionalized surfaces, a calibration curve with a limit of detection of 0.3 μg/mL (21 nM), a dynamic range of 3-50 μg/mL (R^2 = 0.9993) and a sensitivity (slope of the calibration curve) of 17.01 (± 0.32) RU·mL/μg could be constructed for non-aggregated lysozyme.

Selectivity was assessed by challenging the aptasensor with several relevant proteins: cytochrome C (similar size and isolelectric points as lysozyme), myoglobin, bovine serum albumin and with the peptide calcitonin (Supplementary material Table S2 and Figure S1). The response for these proteins was less than 5 % of the signal for the same concentration of lysozyme (30 μg/mL). Interestingly, these proteins have been shown to form amyloid fibrils in vitro[49-52], the MEG-OH surface might therefore be appropriate for such studies too, in conjunction with an adequate biorecognition element.

The aptasensor provides fast response (10 minutes), can be used for repetitive determinations and is simpler compared to ELISA-a classic method based also on biorecognition, which requires several steps and incubation time up to 2 hours with the antibodies[53].

Moreover, the detection limit reported above is better than that of for an impedimetric aptasensor [20] , identical to that of a MIP-based SPR sensor[54] and more than 3 times better than that of previous aptasensor developed by our group[29].

It should be noted that several sensors with significantly higher sensitivity (even with a limit of detection as low as $2x10^{-14}$M), have been developed based on various detection principles, including EIS and SPR[19-21,29, 54-60] (Supplementary material Table S1). Such sensitivity is generally achieved by a more sophisticated design, use of nanomaterials or signal amplification strategies.

For example, for SPR sensors, a 10 pM detection limit was achieved in a competitive test using as a probe a polyclonal antibody with a low dissociation constant (14 pM)[55]. For comparison, dissociation constants in the 2.8 -31 nM range were reported for various lysozyme aptamers in solution[16,18], while in the present study we calculated, by the kinetic titration method[61] a dissociation constant of the immobilized lysozyme aptamer (Kd) of =837 nM. In another SPR sensor, recently described, sensitivity was achieved by modification of SPR interfaces with graphene[21]. Due to the very high surface- to- volume ratio of graphene, and the high capacity displayed by graphene for aptamer imobilization by simple π-stacking interaction, a detection limit of 0.5 nM was reached .

Improving the detection limit of our aptasensor will be the subject of future work. The aptasensor described here is based on a simple design with the main goal of illustrating one of the possible applications of gold interfaces coated with MEG-OH based SAMs.and proving the possibility of following the aggregation process of lysozyme in a specific manner with an aptasensor.

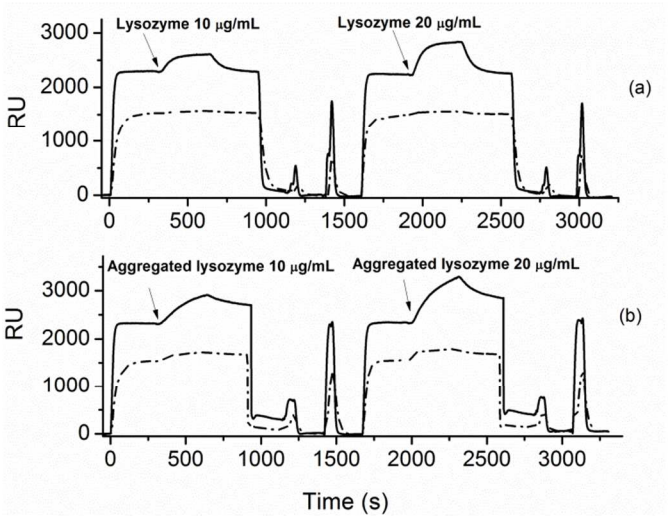

Figure 8. Typical SPR aptasensor response for (top) fresh monomeric lysozyme and (bottom) lysozyme aggregated for 48 h. For each graph, the continuous line corresponds to the measurement of specific binding performed with an aptamer-functionalized surface. The dashed line corresponds to the measurement of NSA on a neutravidin-only control platform.

The SPR response of the aptamer-modified sensor to both lysozyme monomer and oligomers formed after 48 hours of aggregation is shown in Fig. 8 a and b. Notably NSA on neutravidin-only control platforms represented only 5 to 12% of the signal obtained for specific binding on aptamer-modified surfaces. As to be expected, given the alteration in optical mass of an oligomer compared with a monomer, the signal is greater with aggregated species. The slope of the calibration curve in the range 3-50 μg/mL obtained with six solutions of different concentrations of 48 h-aggregated lysozyme was 30 RU·mL/μg, compared to 17 RU·mL/μg for non-aggregated lysozyme. One reason for such behavior is related to the use of mixed thiol matrix, which offers a low–fouling interface. Since the signal obtained with the aptamer is corrected by the non-specific signal, the new coating allows higher absolute responses for aggregate solutions of lysozyme than the previous coating tested, the monomolecular PEG-COOH[29].

Conclusions

SAMs prepared with a recently described monoethylene glycol thiol molecule are shown to be very effective at suppressing the non-specific adsorption of not only lysozyme but also its aggregates, whether the coating was of the monomolecular nature or incorporated a longer, carboxyl-terminated polyethylene glycol thiol cross-linker. It has also been confirmed that the gold substrate cleaning procedure plays a critical role on the resulting SAM protein repelling properties, sodium borohydride being particularly effective to this end. Importantly, low fouling by lysozyme was also displayed by mixed coatings functionalized with neutravidin that were used for the subsequent immobilization of a biotinylated lysozyme aptamer. The SPR-based aptamer sensor thus constructed allowed the detection of lysozyme with a limit of detection of 0.3 μg/mL and a dynamic range of 3-50 μg/mL (R^2 = 0.9993). The mixed PEG-COOH/MEG-OH SAM allowed for low fouling by lysozyme oligomers and fibrils and twice more sensitive specific detection of aggregates as compared to a previous system based on monomolecular PEG-COOH. While the detection limit could be further improved, the high specific SPR signal observed for aggregated lysozyme solutions opens the possibility for a future, more comprehensive study of lysozyme aggregation to be conducted. Additionally, MEG-OH based interfaces could be employed also for other proteins prone to aggregation, with an adequate pair of analyte-biorecognition element.

Acknowledgements

Financial support from Marie Curie International Reintegration Grant FP7 PEOPLE-2010-RG-277126 (for AV) is gratefully acknowledged. Research at the University of Toronto was supported by the Natural Sciences and Engineering Research Council of Canada. This work was supported by grants of the Romanian National Authority for Scientific Research, CNDI – UEFISCDI project numbers PN-II-RU-TE-2011-3-0302 (I.M and VA), PN-II-RU-PD-2012-3-0467 (SD), PN-II-RU-TE-2011-3-0237 (SG), PN-II-RU-TE-2011-3-0076 (BB). We would like to thank Costel Darie (Biochemistry & Proteomics Group, Clarkson University) and Ada Bunea (International Centre of Biodynamics) for manuscript revision, and AFM experiments respectively.

References

1 D.R. Booth, M. Sunde, V.Bellotti, CV. Robinson, WL. Hutchinson, P.E. Fraser, P.N. Hawkins, C.M. Dobson, S.E. Radford, C.C. Blake and M.B. Pepys, *Nature*, 1997, **385**, 787.
2 *E. Frare, M.F. Mossuto, P.P. de Laureto, S. Tolin, L. Menzer, M. Dumoulin, C.M. Dobson and A. Fontana, J. Mol. Biol., 2009, **387**, 17.*
3 Z. Gazova, K. Siposova, E. Kurin, P. Mučaji and M. Nagy, *Proteins*, 2013, **81**, 994.
4 SJ Hyung, AS DeToma, JR Brender, S Lee, S Vivekanandan, A Kochi, J-S Choi, A. Ramamoorthy, BT Ruotolo and MH Lim, *Proc. Natl. Acad. Sci*., 2013, **110**, 3743.
5 M. Gheorghiu , S. David, C. Polonschii, A. Olaru, S. Gáspár, O. Bajenaru, O.B. Popescu and E. Gheorghiu, *Biosens. Bioelectron*. 2014, **52**, 89
6 F. Rahimi, K. Murakami, J.L. Summers, C.-H.B. Chen and G. Bitan, *PLoS ONE*, 2009, **4**, doi:10.1371/journal.pone.0007694.
7 J. Lahiri, L. Isaacs, J. Tien and G.M. Whitesides, *Anal. Chem*., 1999, **71**, 777.
8 D.A. White, A.K. Buell, C.M. Dobson, M.E. Welland and T.P.J. Knowles, *FEBS Lett*., 2009, **583**, 2587.
9 S. Sheikh, J.C.-C. Sheng, C. Blaszykowski and M. Thompson, *Chem. Sci*., 2010, **1**, 271.
10 A. Ulman, *Chem. Rev*., 1996, **96**, 1533.
11 C. Blaszykowski, S. Sheikh, P. Benvenuto and M. Thompson, *Langmuir*, 2012, **28**, 2318.
12 S.-Y. Ow and D.E. Dunstan, *Soft Matter*., 2013, **9**, 9692.
13 E. Frare, P. Polverino De Laureto, J. Zurdo, C.M. Dobson and A. Fontana, *J. Mol. Biol*., 2004, **340**, 1153.
14 S.E. Hill, J. Robinson, G. Matthews and M. Muschol, *Biophys. J.*, 2009, **96**, 3781.
15 M.B. Pepys, P.N. Hawkins, D.R. Booth, D.M. Vigushin, G.A. Tennent, A.K. Soutar, N. Totty, O .Nguyen, C.C. Blake, C.J. Terry, et al. *Nature*, 1993, **362**, 553.
16 D.T. Tran, K.P.F. Janssen, J. Pollet, E. Lammertyn, J. Anné, A. Van Schepdael, and J. Lammertyn, *Molecules*, 2010, **15**, 1127.
17 J.C. Cox and A.D. Ellington, *Bioorg. Med. Chem*., 2001, **9**, 2525.
18 R. Kirby, E.J. Cho, B. Gehrke, T. Bayer, Y.S. Park, D.P. Neikirk, J.T. McDevitt andA.D. Ellington., *Anal. Chem*., 2004, **76**, 4066.
19 Y. Peng, D. Zhang, Y. Li, H. Qi, Q. Gao and C. Zhang, *Biosens. Bioelectron*., 2009, **25**, 94.
20 F. Rohrbach, H. Karadeniz, A. Erdem, M. Famulok and G. Mayer, *Anal. Biochem*., 2012, **421**, 454.

21 P. Subramanian, A. Lesniewski, I. Kaminska, A. Vlandas, A. Vasilescu, J. Niedziolka-Jonsson, E. Pichonat, H. Happy, R. Boukherroub and S. Szunerits., *Biosens. Bioelectron*., 2013, **50**, 239.
22 L.D. Unsworth, H. Sheardown and J.L. Brash, *Langmuir*, 2005, **21**, 1036.
23 M. Mrksich and G.M. Whitesides, A*nnu. Rev. Biophys. Biomol. Struct*., 1996, **25**, 55.
24 P. Harder, M. Grunze, R. Dahint, G. Whitesides and P. Laibinis, *J. Phys. Chem. B*., 1998, **102**, 426.
25 C. Blaszykowski, S. Sheikh and M. Thompson, *Chem. Soc. Rev*., 2012, **41**, 5599.
26 K. Knop, R. Hoogenboom, D. Fischer and U.S. Schubert, *Angew. Chem. Int. Ed.*, 2010, **49**, 6288.
27 L.C. Rosales-Rivera, J.L. Acero-Sánchez, P. Lozano-Sánchez, I. Katakis and C.K. O'Sullivan, *Biosens. Bioelectron*., 2011, **26**, 4471.
28 C. Avci, S. Sheikh, C. Blaszykowski and M. Thompson, *Chem. Commun*., 2012, **49**, 466.
29 A. Vasilescu, S. Gaspar, I. Mihai, A. Tache and S.C. Litescu, *Analyst*, 2013, **138**, 3530.
30 C. Polonschii, S. David, S. Tombelli, M. Mascini and M. Gheorghiu, *Talanta*, 2010, **80**, 2157.
31 A.J. Bard and L.R. Faulkner, 2001. In: Electrochemical methods-Fundamentals and Applications (2nd edn). John Wiley & Sons Inc., NJ, USA
32 BIACORE ® 3000 Instrument Handbook, March 1999, n.d
33 T. Hayashi, Y. Tanaka, Y. Koide, M. Tanaka and M. Hara, *Phys. Chem. Chem. Phys.,* 2012, **14**, 10196.
34 S. Schilp, A. Rosenhahn, M.E. Pettitt, J. Bowen, M.E.Callow, J.A. Callow and M. Grunze, *Langmuir*, 2009, **25**, 10077.
35 L.A. P. Rodríguez-Franco, LI Abad, FX Munoz-Pascual, M Moreno and E Baldrich, *Sens. Actuators B Chem.*, 2014, **191**, 634.
36 S.M. Ansar, F.S. Ameer, W. Hu, S. Zou, C.U. Pittman and D. Zhang, *Nano Lett*., 2013, **13**, 1226.
37 M. Yuan, S. Zhan, X. Zhou, Y. Liu, L. Feng, Y. Lin, Z. Zhang and J. Hu, *Langmuir*, 2008, **24**, 8707.
38 L.M. Fischer, M. Tenje, A.R. Heiskanen, N. Masuda, J. Castillo, A. Bentien, J. Emneus, M. H. Jakobsen and A. Boisen, *Microelectron. Eng*., 2009, **86**, 1282.
39 L. Li, S. Chen, J. Zheng, B.D. Ratner and S. Jiang, *J. Phys. Chem. B*., 2005, **109**, 2934.
40 M.R.H. Krebs, E.H.C. Bromley and A.M. Donald, *J. Struct. Biol*., 2005, **149**, 30.
41 M. Mann, C.K. Meng and J.B. Fenn, *Anal. Chem.*, 1989, **61**, 1702.
42 M. Calamai, J.R. Kumita, J. Mifsud, C. Parrini, M. Ramazzotti, G. Ramponi, N. Taddei, F. Chiti and C.M. Dobson, *Biochemistry (Mosc.).,* 2006, **45**, 12806.
43 C.D. Bain and G.M. Whitesides, *Langmuir*, 1989, **5**, 1370.
44 T. Kakiuchi, M. Iida, S. Imabayashi and K. Niki, *Langmuir*, 2000, **16**, 5397.
45 A. Olaru, M. Gheorghiu, S. David, C. Polonschii and E. Gheorghiu, *Biosens. Bioelectron*., 2013, **45**, 77.
46 S. Sam, L. Touahir, J. Salvador Andresa, P. Allongue, J.-N. Chazalviel, A. C. Gouget-Laemmel, C. Henry de Villeneuve, A. Moraillon, F. Ozanam, N. Gabouze and S. Djebbar, *Langmuir*, 2010, **26**, 809.
47 K. S. Phillips, K. M Kang, L. Licata and N. L. Allbritton, *Lab Chip*, 2010, **10**, 864
48 H. Vaisocherová, V. Ševců, P. Adam, B. Špačková, A. S. Pereira, C. Rodriguez-Emmenegger, T. Riedel, E. Brynda and J. Homola, *Biosens. Bioelectron*., 2014, **51**, 150.
49 N.S. De Groot and S. Ventura, *Spectroscopy* , 2005, 19, 199.
50 M. Fändrich, MA. Fletcher and C.M. Dobson, *Nature*, 2001. **410**, 165
51 N. K. Holm, S.K Jespersen, L.V Thomassen, T.Y Wolff, P. Sehgal, L.A. Thomsen, G. Christiansen, C.B Andersen, A.D. Knudsen and D.E Otzen, *Biochim. Biophys. Acta,* 2007. **1774**, 1128.
52 M. Diociaiuti, M.C. Gaudiano and F. Malchiodi-Albedi, *Int. J. Mol. Sci*., 2011, **12**, 9277
53 Lysozyme ELISA Kit For the in vitro determination of lysozyme in serum, urine and liquor, Manual, ImmunDiagnostik, http://www.immundiagnostik.com/fileadmin/pdf/LYSOZYM_Serum%20Urin%20Liq_1P_K6903.pdf, accessed July4, 2014
54 G. Sener, L. Uzun, R. Say and A. Denizli, *Sens. Actuators B Chem*., 2011, **160**, 791.
55 Bernard, A. Leduc, J. Barbeau, B. Saoudi, L'H Yahia and G. De Crescenzo, *J. Phys. D: Appl. Phys*., 2006, **39**, 3470
56 J. Chen, J. Zhao, J. Jiang and R. Yu, *Talanta*. 2012, **101,** 357.
57 Xie, C. Li, L. Shangguan, H. Qi, D. Xue, Q. Gao and C. Zhang, *Sens. Actuators B: Chem*, 2014, **192**, 558.
58 Y. Xia, S. Gan, Q. Xu, X. Qiu, P. Gao and S. Huang, *Biosens. Bioelectron* 2013, **39** 250.
59 A. Erdem, E. Eksin, M.Muti, *Colloids Surf. B, Biointerf,* 2013, **115C**, 205
60 M. C. Rodriguez, A.-N. Kawde and J.Wang, *Chem. Commun*, 2005, 4267
61 R. Karlsson, P.S. Katsamba, H. Nordin, E. Pol and D.G. Myszka, *Anal. Biochem*., 2006, **349**, 136.

Notes and references

[a] International Centre of Biodynamics, 1 B Intrarea Portocalelor, sector 6, 060101, Bucharest, Romania.
[b] National Institute for Research and Development in Biological Sciences, Bioanalysis Center, 296 Splaiul Independentei, sector 6, Bucharest, Romania.
[c] University of Toronto, Department of Chemistry, 80 St. George Street, Toronto, Ontario, Canada M5S 3H6A
*e-mail: avasilescu@biodyn.ro, tel: +40 (0) 310 4354